International Journal of Physical Sciences Vol. 7(41), pp. 5598-5606, 30 October, 2012
Available online at http://www.academicjournals.org/IJPS
DOI: 10.5897/IJPS12.394
ISSN 1992 - 1950 ©2012 Academic Journals

Full Length Research Paper

The influence of adherend width on tensile strength and failure load of Z joints bonded with adhesive

Bahattin Işcan[1] and Hamit Adin[2]*

[1]Vocational High School of Batman, University of Batman, Batman, Turkey.
[2]Department of Mechanical Engineering, University of Batman, Batman, Turkey.

Accepted 19 July, 2012

In this study, the influence of the adherend width on the tensile strength and failure loads of Z joints were analyzed both experimentally and numerically. The Z joints were subjected to tensile load in the experiments. The stress analyses were executed using the finite element method (FEM). The FEM analyses were performed with Ansys (v.14.0.1). The FEM analyses were carried out to investigate the stress and strain distributions in the adhesive layer of the Z joints. Experimental results were also compared with numerical results, thus they were found quite reasonable. The results showed that the joint strength and failure loads increased when specimen width (b) was increased. Lowest failure load was also determined at the 10 mm width for each specimen. In order to increase the performance of the joint, 30 mm was found to be the most suitable value of width.

Key words: Adhesive, stress analysis, interface, finite element method (FEM).

INTRODUCTION

Adhesive bonding technology is widely used today in almost all the industrial fields of the world and this is mainly due to its high strength–weight ratio, low cost and high efficiency (Hart-Smith, 2005). Adhesive joints supersede, conventional joining methods such as bolting, riveting, soldering and welding from day to day in aviation, space, automotive, substructure, medicine, electronic packaging, sport, building and marine industrials, for which the security of the joints is needed (Apalak and Davies, 1993; Aydin et al., 2004).

Adams and Harris (1973) have studied the influence of the geometry of the ends of the overlap of adhesively bonded joints on the stresses.

The reduction of transverse shear and normal stress concentrations along the edges of adhesive bond-lines is important in order to prevent premature failure of the bonded joint.

Due to differential straining in the substrates, adhesively-bonded joints inevitably experience stress concentrations, especially in the adhesive layer near the ends of overlap where the load transfer takes place (Hart-Smith, 1973; Adams et al., 1997; Kinloch, 1993). A reliable prediction of stresses at locations where a high risk of crack initiation exists is thus a necessary step in designing mechanical structures. Simplified models (Volkersen, 1938; Delale et al., 1981; Gustafson et al., 2007) and solid finite element calculations (Adams and Wake, 1984; Shahin and Taheri, 2007) showed that in adhesive joint, both shear and normal stresses reach their maximum value in the vicinity of the bond edges. These stress concentrations often lead to the joint failure. Different approaches were recently employed to predict the mechanical behavior of bonded assemblies (Goland and Reissner, 1944; Sze´pe, 1966; Pirvics, 1974). Structural designers have developed two different lines of analyses over the years: the strength of materials and fracture mechanics-based methods. The strength of materials approach is based on the evaluation of allowable stresses (Harris and Adams, 1984; Bigwood and Crocombe, 1990) or strains (Crocombe and Adams, 1982; Lee and Lee, 1992), by the FEM. The assembly's strength can be predicted by comparing the respective equivalent stresses or strains at the critical regions, obtained by stress or strain-based criteria, with the

*Corresponding author E-mail: hamitadin@hotmail.com, hamit.adin@batman.edu.tr. Tel: (90-488) 217-3553. Fax: (90-488) 215-7205.

properties of the structure constituents. These criteria are highly mesh dependent, as stress singularities are present at the end of the overlapping regions due to the sharp corners (Qian and Akisanya, 1999; Dragoni and Mauri, 2000; Feih and Shercliff, 2005).

When loaded in the tensile mode of adhesively bonded joints, they developed a linear stress pattern along the bonded overlap. Peak stresses, which may be several times the average failure stresses, are produced at the ends of the lap. Many ideas have been suggested to reduce the high stresses that occur at the ends of the overlap. Geometrical modifications involve altering the shape of the adherend and/or adhesive. Among these methods are pre-formed adherends, taper, fillets, rounding, adherend shape optimization, etc. (Sancaktar and Nirantar, 2003).

A method for making the shear stress uniform along the bond length was presented by Cherry and Harrison (1970). The tensile strains on both adherends were set equal to each other at each point by modifying the adherend thickness. It was assumed that the displacements through the thickness of the adhesive were negligible; the adhesive layer was thin enough so that the edge effects could be ignored, and the bond length was much greater than the adherend thickness. The ideal adherend profile for making the shear stress uniform was found to be a symmetric taper of the adherend along the bondline. In addition to being a function of the adherend thickness, the shear stress was also a function of the Young's modulus of the adherends.

Işcan et al. (2011) investigated stress analysis of bonded Z type that connected with various adhesives. The results showed that the maximum values of stress occurred at the middle section of the joints, whereas the minimum values of stress occurred at the edges. Furthermore, geometrical exchange has considerable effects on maximum stresses, dependent upon the load.

In this study, the mechanical behaviors of bonded Z joints using adhesive under a tensile load was analyzed. Tensile experiments on the Z joints with different adherend width were carried out. The FEM calculations were performed via Ansys (2011, v.14.0.1). The effects of adherend width on adherends stress and strain at the interfaces were investigated. Failure loads of the Z joints were examined as both experimental and FEM results. Experimental results were also compared with the FEM results.

EXPERIMENTAL METHOD

Determination of mechanical properties of adhesive

The stress–strain (σ –ε) behaviors of the adhesive was determined by bulk specimens tested under specified conditions. The bulk specimens used in this study were prepared according to ISO 15166-2 (ISO 15166-2, 2000) as described by Temiz (2006) and Temiz et al. (2005).

The experiments of bulk specimen were performed using video extensometer, Shimadzu (Shimadzu Corporation, Tokyo, Japan) (250 kN) machine at room temperature and relative humidity 50%±5. During tensile tests, the crosshead speeds were maintained at 1 mm/min. Four specimens were tested. Typical tensile stress–strain curve for the adhesives is shown in Figure 1. Upon reaching the peak of stress, the stress dropped suddenly and the bulk specimen experience failure (Adin, 2012a, b). When noting the results of Figure 1, the stress–strain curve is nearly linear. Hence, adhesive has showed linear elastic behavior. It can be seen in Figure 1 that the maximum stress of the adhesive is measured as 72 MPa.

Mechanical properties of adhesive and adherend was shown in Table 1. It is clearly seen from Table 3 that Young's modulus and Poisson's ratio of the 2214 regular type adhesive were 5171 MPa and 0.35, respectively.

Production of the Z joints

In the study, the 2214 regular adhesive produced by 3M was chosen as adhesive and steel ($Fe_{49}Cr_{15}Mo_{14}C_{18}B_3Er_1$) was utilized as adherend. The dimensions of adherend and adhesive are shown in Table 2 and Figure 2. Young's modulus and Poisson's ratio of adherend are 210 GPa and 0.32, respectively. The thicknesses of adhesive and adherend were chosen as 0.20 and 5 mm, respectively. In addition, the overlap angle of adherend was chosen as 45°. The other dimensions are shown in Figure 2. Since effects of adherend width were examined, the same element dimension was used in all models as often as practicable. The upper and lower cover plates have the same dimensions and materials.

Five different adherend width and overlap length were used. The Z joints were manufactured as four different specimens for each condition of adherend width. The mechanical properties of adherend and adhesive are given in Table 1. Before bonding, the adherend surfaces were degreased with acetone, etched with H_2SO_4+ $Na_2Cr_2O_7.2H_2O$ for 30 min at 60-65°C, washed in running tap water and dried in an oven for 30 min at 60°C. Then, the adhesive was prepared and then applied at the joint surface and the adherend were clamped for curing as cure of adhesives were waited.

Experiments of the Z joints were performed under the same conditions with bulk specimen experiments as mentioned above.

FINITE ELEMENT MODELLING OF THE Z JOINTS

In this step, finite element method (FEM) was employed in order to analyze the behaviors of the Z joints. The FEM calculations were the ANSYS (Academic Teaching Advanced, Ver. 14.0.1) software. Additionally, the stress-strain analysis was obtained according to von Mises yield criterion. Gali et al. (1981) showed that the von Misses yield criterion was suitable to model the stress-strain behavior of the adhesives used in the joint. By means of this criterion, the stress-strain distributions in the adhesive layer were calculated.

Loading, boundary conditions and mesh conditions were presented in Figure 2 (Işcan et al. 2011). Solid 45 elements were used. The elements are composed of eight different nodes with two degrees of freedom.

Çolakoğlu and Apay (2012) showed that if the mesh density along the transverse direction of the overlap was greater than 3 elements per mm, then the variation in maximum principal stress and von Mises stress with mesh density would be effectively removed.

The mesh density can effect the strain predictions in the adhesive layer. A smaller element size will generally give a higher strain. For this reason, the size of elements in the mesh was

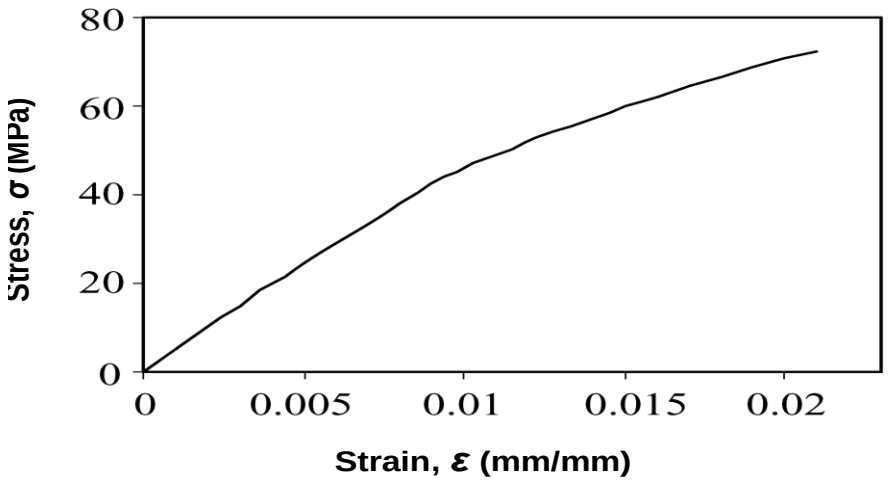

Figure 1. Tensile stress–strain behaviors of 2214 adhesive (Temiz, 2006).

Table 1. Material properties of the adherend and adhesive.

Parameter	Adherend (Steel) (Işcan et al., 2011)	Adhesive (2214) (Temiz, 2006)
E (MPa)	210.000	5171
v	0.32	0.35
σ^* (MPa)	410	72

E, Young's modulus; *v*, Poisson's ratio; σ^*, ultimate strength.

Table 2. Geometrical parameters of the Z joints used in experimental and numerical studies (all dimensions in mm).

Adherend width (mm)	Adherend thickness (t) (mm)	Overlap length (a) (mm)	Overlap length (b) (mm)	Overlap angle	Adhesive thickness (n) (mm)
10	5	45	25	45°	0.20
15	5	45	25	45°	0.20
20	5	45	25	45°	0.20
25	5	45	25	45°	0.20
30	5	45	25	45°	0.20

Table 3. Experimental and calculation failure loads and ultimate stresses.

Adherend width (mm)	σ_E (MPa)	σ_{FEM} (MPa)	S_Q	F_E (kN)	F_{FEM} (kN)	F_R
10	67.923	71.955	0.9439	3.39614	3.59775	0.9439
15	69.315	72.001	0.9627	5.19862	5.40008	0.9626
20	69.587	72.071	0.9655	6.95872	7.20710	0.9655
25	69.691	72.149	0.9659	8.71138	9.01863	0.9659
30	70.482	72.597	0.9709	10.57323	10.88955	0.9708

σ_E; Experimental stress, σ_{FEM}; FEM stress, $S_Q = \sigma_E / \sigma_{FEM}$ (Finite element analysis stress/Experimental stress), F_E; Experimental damage load of adhesives; F_{FEM}: Damage load predicted from FEM adhesives; $F_R = F_E / F_{FEM}$ (Finite element analysis load/experimental load).

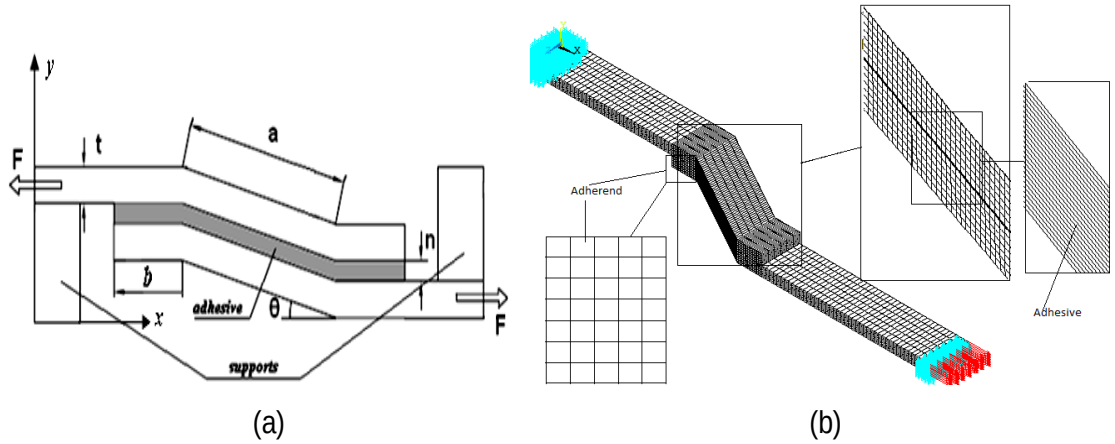

Figure 2. Configuration of specimens under load: (a) geometry; (b) Mesh details and boundary conditions (Işcan et al. 2011).

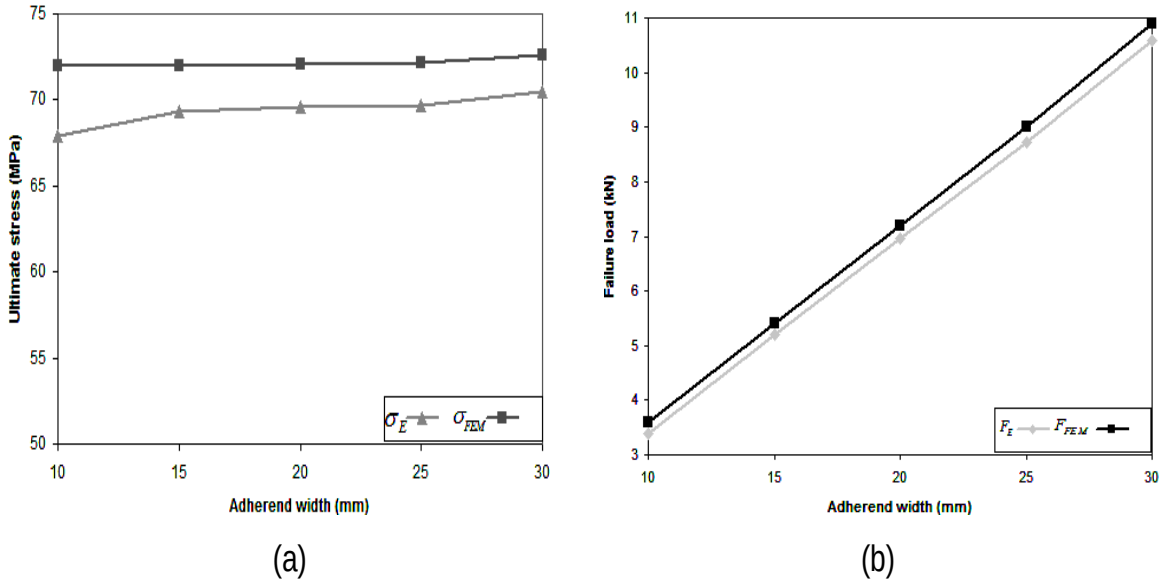

Figure 3. Comparison of experimental value and FEM value; a) ultimate strength b) failure loads.

reduced until a stable strain value had been achieved. Eventually, 25 elements through the adhesive thickness (0.20 mm) were used in the models,as shown in Figure 3b. The adherend thickness and width were meshed with 7 and 6 layers, respectively. So, the smallest element sizes were used as 0.008 mm in the adhesives and 0.7143 mm in the adherends. The total number of nodes and elements were chosen 26656 and 21630, respectively.

RESULTS AND DISCUSSION

Experimental results

Three different Z joints were tested in the experiments for each conditions of adherend width. The specimens of the Z joint were carefully and closely observed to understand failure mechanism during the tensile experiments. All failures of the joints were catastrophic failure and at the adhesive interface without breaking the adherends. The average value of failure loads are presented in Table 3. It is clearly seen from Table 3 that the lowest failure load was determined at the 10 mm width for each specimen. The failure loads of the joint with 2214 regular adhesive obtained from experiments are given in Figure 4.

It can be seen from Figure 3 that when the adherend widths were increased, the failure loads and ultimate stresses increased as well. Hence, increase in width has

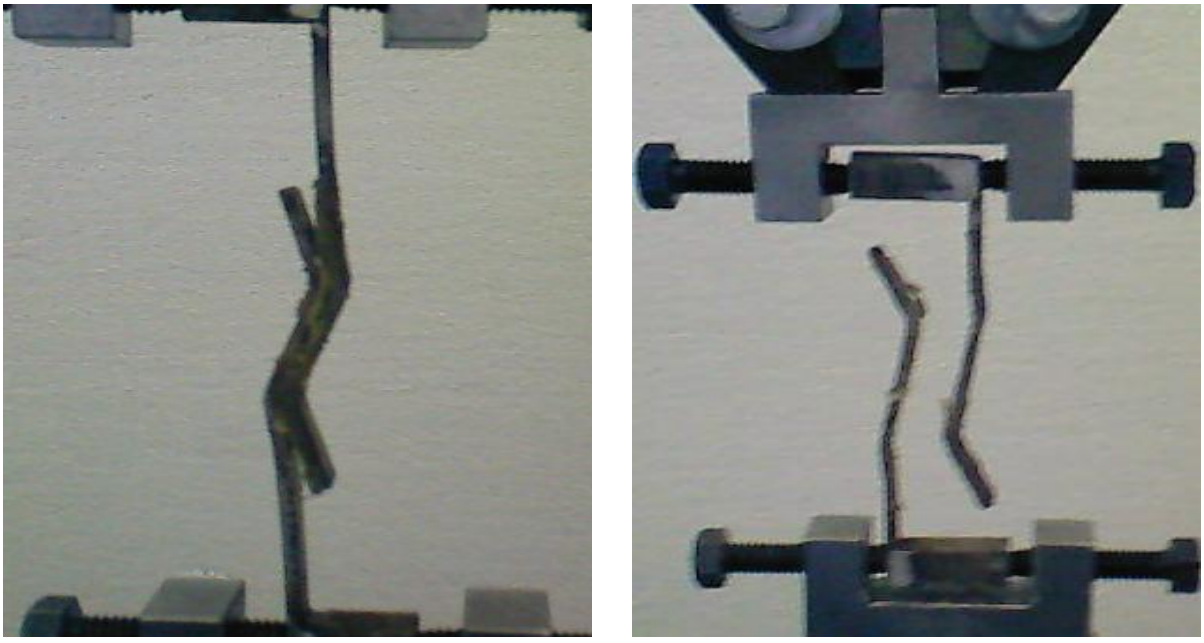

(a) (b)

Figure 4. Experiments of the Z joints; a) peeling in an adhesive region b) rupture an adhesive region.

effect on the failure load with 2214 adhesive. The adherend widths played a significant role in failure initiation and loads. So, the adhesion area of overlap length increased gradually with an increase in adherend width, therefore, the failure load increased. In Figure 4a, we can confirm that experimental and calculation stresses are almost same. These suggest that the stresses must be dependent to adherend width.

Figure 4 shows examples of experimental photos of the Z joints. Obviously, fairly peeling of free edges was realized as can be seen from this figure. Failure initiation most likely occurred at edges of the overlap within the interface of the adhesives. The failures at both free ends propagate towards the center of overlapping region.

The FEM results and comparison with experimental results

The solution in the FEM considering linear material behavior is reached by dividing the total load in steps to track the equilibrium paths and iterating to a converged solution at each load increment.

To find out the failure loads of the specimens in the FEM calculations, ultimate strength of adhesive (σ^*) was used. The σ^* value of adhesive was measured as 72 MPa (Figure 1). The equivalent stress (σ_{eqv}) was calculated using the von Mises failure criterion and it was assumed that the failure occurred when the equivalent stress calculated at any point of the adhesive layer reached the ultimate strength of adhesive. In addition, the effects of width at the interfaces of adherend were examined.

As the maximum von Misses stress values at adhesive interface approach to these values, then, they were multiplied with the frontal area of specimens (t × b = thickness of specimen × width of specimen) from which the failure loads those seen in Table 3 were obtained. From Table 3, the failure load values of FEM calculations and the experimentally measured failure loads seem to be quite close to each other. In the last columns of the table, the convergence ratios were found by dividing the experimental loads (F^*_E) with failure loads (F_{FEM}) obtained using FEM calculations. In general, the values of F_R were found to be very close to 1. As a result, the experimental failure loads were consistent with the failure loads of FEM calculations. Same method was used to observe the effects of width on the stresses. Furthermore, the stress ratios (S_Q) were found close to 1.

Sümer and Aktaş (2011) investigated that numerical and experimental results showed very good agreement in terms of the load-deflection, load-strain relationships.

Consequently, a fairly good agreement is observed between the FEM results and experimental results (Table 3 and Figure 3). In addition to, ratio values are found to be very close to 1. Therefore, failure initiation may probably occur at edges of overlap length at interface of the adhesive, as in Figure 4. Then, the failure at both free

ends promote to the centre of overlap before joining each other.

Effect of the adherend width on stress distribution

The stress distributions along the overlap length for different adherend width obtained from FEM analysis is presented in Figure 4. The σ_x stress and σ_y peel stress distributions along the overlap length for different adherend width are given in Figure 4 (a), and (b), respectively. The σ_x and σ_y stresses were maximum at the edges of overlap length. The stresses increased when close to free edges. In addition, σ_x and σ_y increased with increasing of adherend width. Note that both the σ_x and σ_y stresses were symmetric along the horizontal centerlines of the adhesive.

The shear stress (τ_{xy}) and equivalent stress (σ_{eqv}) distributions along the overlap length for different adherend width are depicted in Figure 5c, and d, respectively.

The τ_{xy} was minimum at the edges of overlap length, whereas it was maximum in the middle of overlap length. The σ_{eqv} was symmetric and maximum at the edges of overlap. The σ_{eqv} stress also increased when the adherend width increased. The shear stress τ_{xy} was symmetric. σ_x, σ_y and σ_{eqv} were maximum at the edges of overlap. They were more uniform at the end of the overlap length. The comparison indicates close agreement for the stress distribution of σ_x, σ_y and σ_{eqv} as shown in Figure 5a, b, and d, respectively. Both the peeling and shear stresses were increased with increasing of adherend width. Due to these stresses, failures were initiated at the edges of overlap. This situation was seen in the same manner as in Figure 4. The reason of this is that when the adherend width gets thinner, the adhesive in the butt region is exposed to more strain in the loading direction and this causes an increase in the normal and equivalent stresses.

The present FEM calculation and experimental results have shown that the most critical points are along the adherend-adhesive interfaces and the σ_x, σ_y and σ_{eqv} stresses are located between the centerline and at the opposite corner ends of overlap. For this reason, the bondline on the adhesive side was taken into consideration for the stress analysis and all of the stresses (σ_x, σ_y, τ_{xy}, and σ_{eqv}) distributions were normalized.

Figure 5d indicates that more shear stress is transferred towards the end from the centre of the overlap with increasing adherend width, due to reduced elastic deformations on the adhesives. Therefore, the effect of shear stress on the failure and strength of the adhesively bonded joints increased. Similarly, it is evident that more equivalent stress is transferred towards the end from the centre of the overlap with increase in overlapping length, as seen from Figure 5c.

Effect of the adherend width on strain distribution

The strain distributions along the overlap length for adherend width are illustrated in Figure 6. The ε_x, ε_y, γ_{xy} and ε_{eqv} distributions along the overlap length are given in Figure 6a, b, c and d, respectively. The ε_y and ε_{eqv} strains were maximum at the ends of the overlap. The strain of ε_y was decreased with increase of the adherend width along overlap length. Contrarily, the equivalent strains (ε_{eqv}) were increased. The ε_x strain was maximum in the middle of overlap length, and was increased when far from edges. Figure 6c showed that the adherend width had a considerable effect on γ_{xy} strain distributions, and the values of γ_{xy} were increased when the adherend width was increased. Maximum and minimum values of the shear strain were obtained in edges and middle of overlap length. It can be seen from Figure 6a and c that the strains were increased when the overlap length was increased. In addition, note that the ε_x, ε_y, γ_{xy} and ε_{eqv} strain distributions were symmetric along the x-y axis. All of the strains were maximum at the ends of the overlap length except for ε_x strain.

When the magnitude of the equivalent stress and strain is considered, it is clear that the equivalent stresses have very important influence on the initiation and propagation of failure at the edges of the Z joints. Consequently, failure initiation probably occurred on the edges of overlap length at the interface of adhesives. Then, the failure at the ends of the overlap promotes the centre of the overlap before joining each other.

Von Mises contour stress and strain distribution of FEM is shown in Figure 7. It is clearly seen that the maximum values of equivalent stress and strain were at middle sections of the overlap length. All contours were examined, and it was observed that the values of normal and equivalent stress and strains increased with increase of adherend width.

Conclusions

This work studied the effects of adherend width on Z joints subjected to static tensile loadings. Finite element method (FEM) was used for the calculations, and the following results were obtained:

1) There was a fairly good agreement between the experimental and FEM calculation results. This harmony was realized between both the failure loads and the ultimate stresses.
2) Failures were realized at the adhesive interface; the adherend widths were affected by the loads of failure, and the lowest failure load was determined at the 10 mm

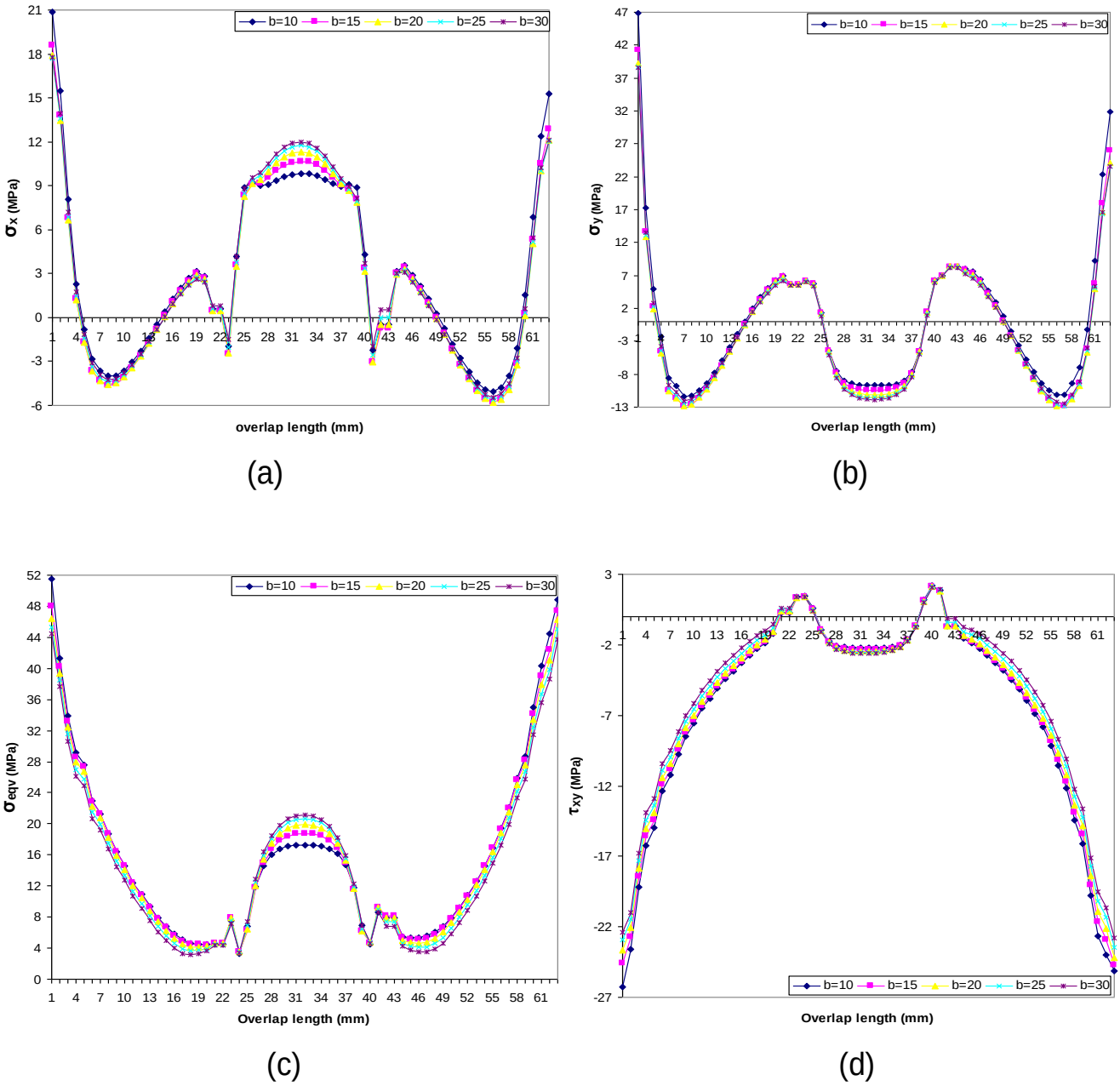

Figure 5. Stress distributions throughout overlap length: (a) σ_x stress distributions; (b) σ_y stress distributions; (c) σ_{eqv} stress distributions; (d) τ_{xy} shear stress distributions.

width for each specimen.

3. The stress and strains changed depending on the adherend width; when adherend width increased, the values of normal and equivalent stress and strains also increased.

4. The stresses and strains were symmetric along the overlap length. Furthermore, equivalent stresses and strains were greatest at the edge of overlap, whereas shear stress and strain were smallest.

5) The peeling and shear stresses increased with an increase in adherend width. Due to these stresses, failures were initiated at the edges of overlap. The reason for this is that when the adherend width gets thinner, the adhesive in the angle region gets exposed to more strain in the loading direction, and this causes an increase in the normal and equivalent stresses.

6) Shear and equivalent stresses and strains were transferred towards end from the centre of the overlap

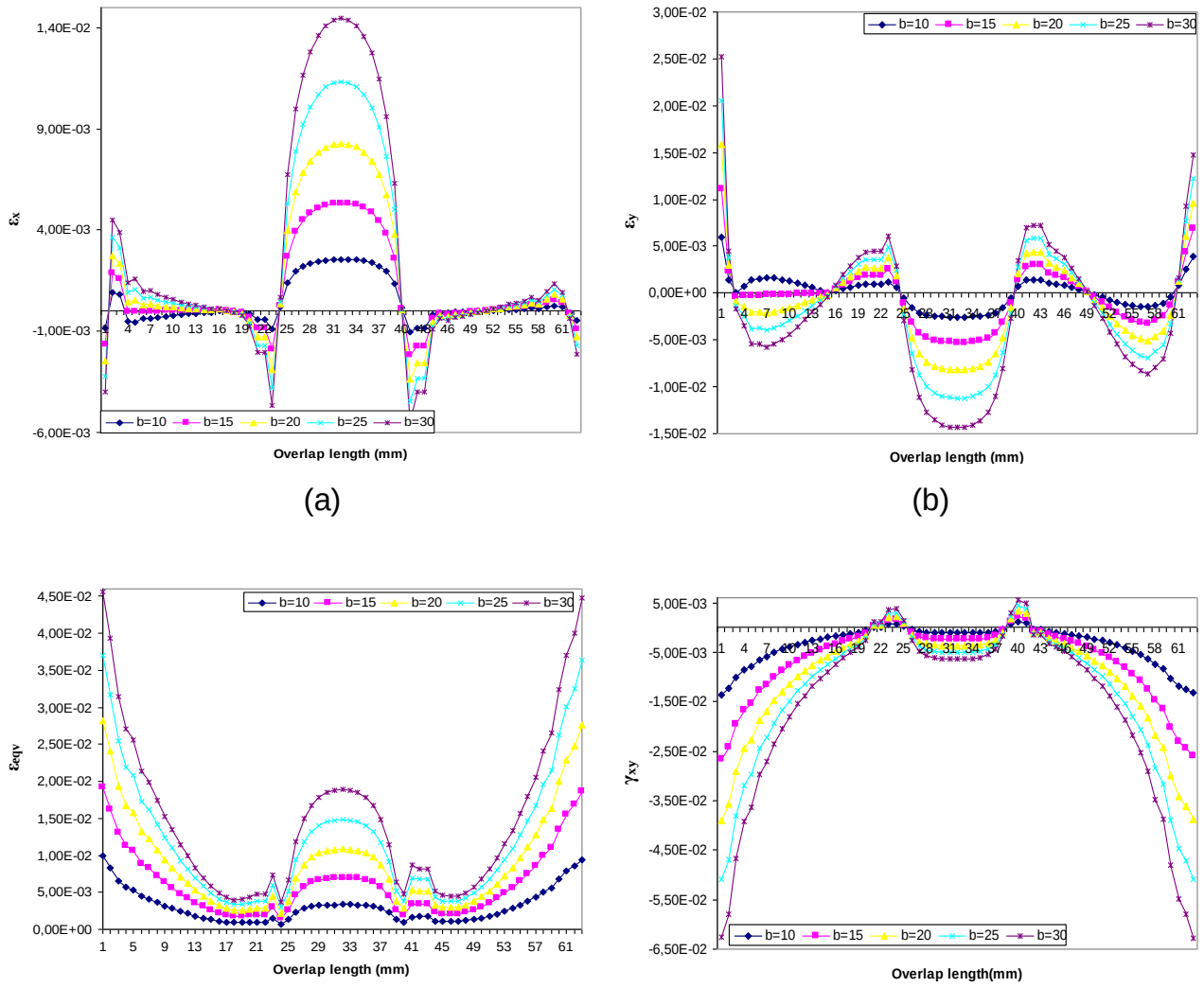

Figure 6. Strain distributions throughout overlap length: (a) ε_x strain distributions; (b) ε_y strain distributions; (c) ε_{eqv} strain distributions; (d) γ_{xy} shear strain distributions.

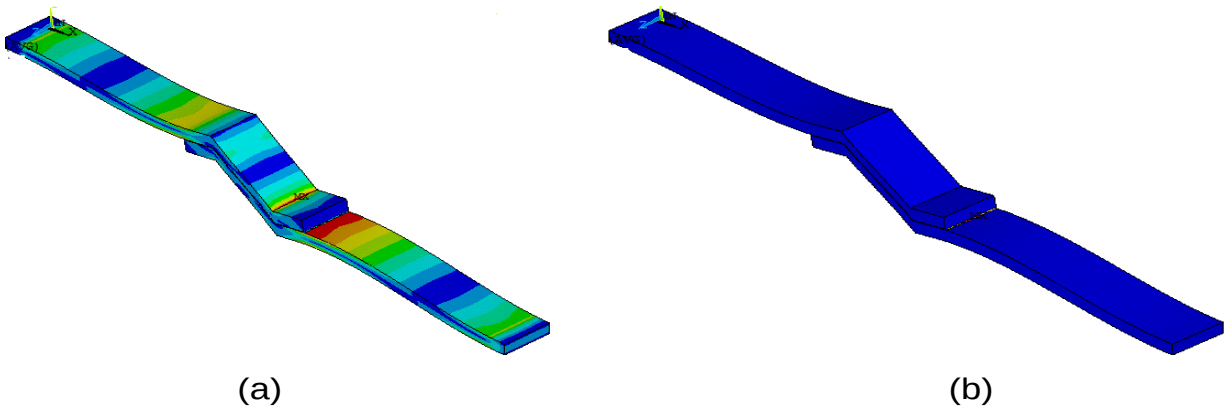

Figure 7. Von Mises stress (a) and strain (b) contour distributions obtained from 3-D FEM for 2214 adhesive.

with increasing adherend width, due to the reduction in the elastic deformations on the adhesives.

REFERENCES

Adams RD, Wake WC (1984). Structural adhesive joints in engineering London: Applied Science Publications. p. 440

Adams RD, Comyn J, Wake WC (1997). Structural Adhesive Joints in Engineering. Elsevier. Amsterdam. pp. 281-285.

Adams RD, Harris JA (1987). The influence of local geometry on the strength of adhesive joints. Int. J. Adhes. Adhes. 7:69–80.

Adin H (2012). The effect of angle on the strain of scarf lap joints subjected to tensile loads. Appl. Math. Model. 36:2858-2867.

Adin H (2012). The investigation of the effect of angle on the failure loads and strength of scarf lap joints. Int. J. Mech. Sci. 61:24-31.

ANSYS (2011). Academic Teaching Advanced, 14.0.1, The general purpose finite element software. Swanson Analysis Systems. Houston. TX.

Apalak MK, Davies R (1993). Analysis and design of adhesively bonded corner joints. Int. J. Adhes. Adhes. 13:219-235.

Aydin MD, Temiz Ş, Özel A (2004). Yapısal yapıştırıcıların mekanik özelliklerinin belirlendiği deneysel yöntemler. Mach. Eng. 536:18-24.

Bigwood DA, Crocombe AD (1990). Non-linear adhesive bonded joint design analyses. Int. J. Adhes. Adhes. 10:31-41.

Cherry BW, Harrison NL (1970). The Optimum Profile for a Lap Joint. J. Adhes. 2:125-130.

Çolakoğlu MH, Apay AC (2012). Finite element analysis of wooden chair strength in free drop. Int. J. Phys. Sci. 7(7):1105-1114.

Crocombe AD, Adams RD (1982). An elastoplastic investigation of the peel test. J. Adhes. 13:241-267.

Delale F, Erdogan F, Aydinoglu MN (1981). Stresses in adhesively bonded joints: a closed form solution. J. Compos. Mater. 15:249-259.

Dragoni E, Mauri P (2000). Intrinsic static strength of friction interfaces augmented with anaerobic adhesives. Int. J. Adhes. Adhes. 20:315-321.

Feih S, Shercliff HR (2005). Adhesive and composite failure prediction of single-L joint structures under tensile loading, Int. J. Adhes. Adhes. 25:47-59.

Gali S, Dolev G, Ishai O (1981). An effective stress/strain concept in the mechanical characterization of structural adhesive bonding. Int. J. Adhes. Adhes. 1:135-140.

Goland M, Reissner E (1944). The stresses in cemented joints. J. Appl. Mech. 66:17-27.

Gustafson PA, Bizard A, Waas A (2007). Dimensionless parameters in symmetric double lap joints: An orthotropic solution for thermomechanical loading. Int. J. Solids Struct. 44:5774-5795.

Harris JA, Adams RD (1984). Strength prediction of bonded single-lap joints by non-linear Finite Element Methods. Int. J. Adhes. Adhes. 4:65-78.

Hart-Smith LJ (1973). Adhesive-bonded Single-lap Joints, NASA Technical Report CR-112236. NASA. Houston.

Hart-Smith LJ (2005). Aerospace, In: Adams RD, editor. Adhesive bonding. Cambridge England: Woodhead Publishing Ltd. pp. 489-494.

Işcan B, Adin H, Turgut A (2011). The effect of overlap length adhesive with bonded in Z type materials. Int. J. Phys. Sci. 6(15):3619-3627.

ISO 15166-2 (2000). Adhesives-methods of preparing bulk specimens. Part 2: Elevated-temperature-curing one-part systems.

Kinloch AJ (1993). Adhesion and Adhesives. Chapman and Hall. London. pp. 311-313.

Lee SJ, Lee GL (1992). Development of a failure model for the adhesively bonded tubular single lap joint. J. Adhes. 406:1-14.

Pirvics J (1974). Two dimensional displacement-stress distributions in adhesive bonded composite structures. J. Adhes. 6:207-228.

Qian ZQ, Akisanya AR (1999). An investigation of the stress singularity near the free edge of scarf joints. Eur. J. Mech. A/Solids. 18:443-463.

Sancaktar E, Nirantar P (2003). Increasing strength of single lap joints of metal adherends by taper minimization. J. Adhes. Sci. Technol. 17:655-675.

Shahin K, Taheri F (2007). Analysis of deformations and stresses in balanced and unbalanced adhesively bonded single-strap joints. Compos. Struct. 81:511-524.

Sümer Y, Aktas M (2011). Bond length effect of fiber reinforced polymers bonded reinforced concrete beams. Int. J. Phys. Sci. 6(24):5795-5803.

Sze´pe F (1966). Strength of adhesive-bonded lap joints with respect to change of temperature and fatigue. Exper. Mech. 6:280-286.

Temiz Ş, (2006). Application of bi-adhesive in double-strap joints subjected to bending moment. J. Adhes. Sci. Tec. 20:1547-1560.

Temiz Ş, Özel A, Aydin MD (2005). The effect of adherend thickness on the failure of adhesively-bonded single-lap joints. J. Adhesion Sci. Tec. 19(8):705-718.

Volkersen O (1938). Dienietkraftverteilung in zugbeanspruchten mit konstanten laschenquerschnitten. Luftfahrtforschung 15:41-47.